Application of a 3D numerical model to a river with vegetated floodplains

T. Stoesser, C. A. M. E. Wilson, P. D. Bates and A. Dittrich

ABSTRACT

This paper describes the application of a three-dimensional computational fluid dynamics code to a large-scale river scheme. One of the primary aims of this paper is to provide a tool, which utilises a roughness closure derived from physical processes, requiring minimal calibration. Accordingly, a roughness closure based on the traditional drag-force approach is implemented. Unlike other implementations of this approach, the drag force is only introduced in the momentum equations and not into the turbulence closure. This ensures that the coefficients of the turbulence closure model (in this case the $k-\epsilon$ scheme) do not require recalibration for each application. An existing vegetated floodplain is used as a reference site and parameters characterising the dimensions of riparian vegetation and its distribution are quantified. A 100 year flood event on a considerable reach length (3500 m) of the lower River Rhine in South-West Germany is then simulated. Mean floodplain velocities are measured using dilution gauging techniques and these are compared with the computed values. Given information such as plant distribution and geometric properties of the various plant populations, the proposed tool can predict floodplain velocities, water elevation and hydrodynamic features indicative of vegetated compound channel flow.

Key words | flood modelling, vegetation, river restoration, two-stage channels

T. Stoesser (corresponding author)
Numerical Methods for Turbulent Flows,
Institute for Hydromechanics,
University of Karlsruhe,
D-76128 Karlsruhe,
Germany
Tel: +49 721 608 3533;
Fax: +49 721 606 046
E-mail: *Stoesser@ifh.uka.de*

C. A. M. E. Wilson
Cardiff School of Engineering,
Division of Civil Engineering,
Cardiff University, Queen's Buildings,
The Parade,
ENGIN 1, PO Box 925,
Cardiff CF24 0YF,
UK

P. D. Bates
School of Geographical Sciences,
Bristol University, University Road,
Bristol BS8 1SS,
UK

A. Dittrich
Leichtweiss Institut für Wasserbau,
Universität Braunschweig,
Abt. Wasserbau und Gewässerschutz,
Beethovenstrasse 51a,
38106 Braunschweig,
Germany

INTRODUCTION

River restoration is the repairing of a degraded ecosystem to a close approximation of its natural state. Often the enhancement of a riverine environment is carried out for several purposes including increasing the river system's conveyance capacity, the creation of floodwater retention, the enhancement of water quality and the improvement of wildlife habitat. Both aquatic and riparian vegetation have become central to river restoration schemes and the importance of their preservation to river ecology is now recognised. The reinstatement of vegetation will diminish the river's conveyance capacity, although its presence and associated reduction in mean velocity is necessary to provide habitat for invertebrate communities, and fish spawning grounds. Furthermore recent bioengineering approaches, which combine both live and dead plants to produce natural functioning systems, have been used to prevent and control erosion, and to enhance natural decontamination of agricultural runoff entering the river system.

This is an area in its infancy and few recommendations are available to aid the practitioner to assess the impact of meander, floodplain and, in particular, vegetation reinstatement both on the local velocity distribution and the flood conveyance of the system. In the past, vegetation in open channels was treated as an additional flow resistance to be added to the bed roughness (see Cowan 1956; Chow 1959) in one-dimensional flow formulae, since submerged and emergent riparian vegetation may be considered to be the fundamental source of energy loss in natural compound channel flow. A similar one-dimensional method was later followed by Petryk & Bosmaijan (1975), who developed an approach to account

Downloaded from https://iwaponline.com/jh/article-pdf/5/2/99/392567/99.pdf
by guest

for varying flow depths and vegetative characteristics. Due to varying depth and flow resistance along the width of a compound channel, the determination of discharge capacity can be complicated. Overbank areas have to be subdivided into different regions that have different roughness properties to the main channel. Many variations of the divided channel method have been proposed (see, for example, Masterman & Thorne 1982; Greenhill & Sellin, 1993). Typically the compound cross section is subdivided into sub-regions accounting for the depth/resistance variation. However, some approaches also account for the turbulent momentum exchange between the faster velocities in the main channel and the slower velocities on the vegetated floodplain (Wormleaton *et al.* 1982; Ervine & Ellis 1987).

More complex methods for multi-dimensional flow problems have been developed by Shimizu & Tsujimoto (1994) and Lopez & Garcia (1997) using a two-equation turbulence closure approach. This was first introduced by Wilson & Shaw (1977), to model atmospheric flows over plant canopies. A modified $k-\varepsilon$ turbulence closure model is used, introducing drag-related sink terms into the momentum as well as into the turbulent transport equations. Experiments conducted at the Hydraulic Laboratory, Kanazawa University, Japan (Tsujimoto *et al.* 1991) have been used to validate the model. Shimizu & Tsujimoto calibrated their model by adjustment of the two additional turbulence constants that appear in the two-equation closure to reproduce observed mean velocities and Reynolds stresses. Lopez & Garcia conducted similar experiments and modified the same weighting factors of the $k-\varepsilon$ model but reported calibrated values, which differed by about 500% from those of Shimizu & Tsujimoto. More recently, Choi & Kang (2001) have used a higher-order closure, a Reynolds stress model, to simulate the flow through rigid vegetation elements in a flume study. This was tested against laboratory data for one vegetation and flow condition. Whilst higher-dimensional approaches are appropriate for reproducing laboratory experiments, their need for recalibration for each vegetation/flow condition is a serious disadvantage for practical applications. In order to overcome this we here report the application of a 3D numerical code with a drag-force roughness closure that does not require recalibration of the turbulence closure scheme and should thus prove to be more general than previous approaches. This model is applied to flow in the vegetated two-stage channel of a 3500 m reach of the lower River Rhine, Germany.

BACKGROUND

This study is based on an agreement made between the Federal Republic of Germany and France in 1982, which had two main objectives. First, it aimed to re-establish flood protection for the River Rhine for a 200 year flood event. Second, and of equal importance, it aimed to re-instate a wetland and freshwater environment rich in species diversity. Previously, the upper reach of the Rhine had been dam-regulated and this had not only reduced its flood conveyance capacity but also caused a considerable decline in both aquatic species and plant communities. A preliminary solution to satisfy both of these aims was to erect a retention weir in the river and use some of the former floodplains to give a total storage volume of 53 million m^3. However, extensive investigations indicated that this volume was not sufficient to guarantee flood protection for a 200 year flood event. Consequently, a project called 'The Integrated Restoration Project at River Rhine' was initiated in 1983 in order to refine and improve this approach further.

This project proposed that, in order to overcome the deficit in flood storage, that all former floodplains be restored to attain an additional retention volume of 25 million m^3. This task may be accomplished by the re-instatement of an additional floodplain on a 40 km reach between Märkt and Breisach in the southwest of Germany, where the average floodplain width is approximately 90 m. However, one of the primary requirements of the brief was that flood protection was to be fulfilled in an ecologically sensitive manner, and to establish a sustainable riverine ecosystem, which was not dependent on high maintenance in the future.

The design storage volume can only be achieved by the establishment of a pre-designed water level along the reach during a flood event. This water level can only be

Downloaded from https://iwaponline.com/jh/article-pdf/5/2/99/392567/99.pdf
by guest

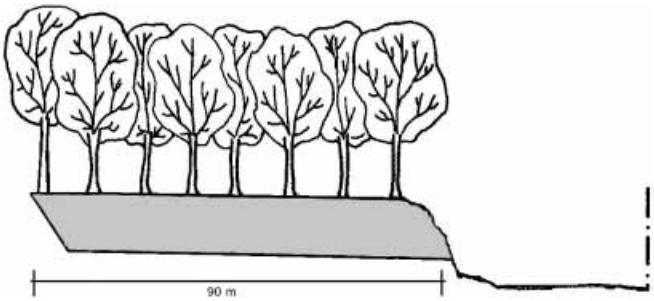

Figure 1 | Typical cross section of the present situation with the intended floodplain area to be dredged (grey).

attained by considerably higher roughness on the new re-instated floodplains than in the main channel, e.g. riparian forest vegetation. Secondary to providing a flood retention volume, it was necessary to ensure that the floodplains are designed in such a manner to damp both the propagating floodwave front and its recession. After dredging (see Figure 1), the floodplains will be covered with fine sediments and exposed to high shear stresses. This is especially problematic in the case of a stormwater event, where massive erosion would take place and prevent establishment of new species. Thus, an integrated hydraulic and ecological approach is necessary to establish both the magnitude of hydraulic resistance necessary to attain the desired retention capacity and the corresponding type of vegetation necessary to fulfil this task. Furthermore it is necessary to predict the resulting floodplain flow properties and to assess whether these flow conditions are appropriate for the natural establishment, preservation and succession of the riparian flora and fauna.

Existing knowledge of river dynamics in riparian forests cannot provide the necessary information to give insight into all technical and ecological issues, so one of the main aims of the Integrated Restoration Project was to provide recommendations for the management of such environments. Central to the project is the accurate prediction of the flow field in and around riparian vegetation and this is the facet of the Integrated Rhine Restoration project reported herein.

METHODOLOGY

In order to achieve these integrated objectives, a 3D numerical model developed at Bristol University (Stoesser 2002) was applied to relevant reaches of the Rhine. A 3D approach was considered appropriate in order to capture the variation in streamwise and cross-streamwise velocity with depth, induced by both channel curvature, natural bed forms and riparian vegetation, and also the high velocity gradients generated by the changes in the cross-sectional flow area. Furthermore, as we wish to simulate flows through riparian floodplain forests, traditional roughness closure methods are somewhat inadequate. These use a 1D resistance formula, which is usually calibrated by adjustment of a roughness coefficient until the model output reproduces the observed hydraulic behaviour as accurately as possible. However, this process of calibration lumps together a number of resistance effects, skin friction and form roughness, turbulence, multi-dimensional flow effects, etc., into a single term. Moreover, a 3D representation of flow velocities, local bed-shear stresses and hydrodynamic forces are preferable as model output in order to evaluate the floodplain flow scenario in terms of flood protection, ecology and geomorphology. A multi-dimensional model with a physically based roughness closure approach for vegetative resistance which involves a minimum of parameter calibration is therefore required and has thus been developed and implemented within the new model. The method used is derived from a traditional drag-force approach whereby the vegetational elements are treated as obstructions to the flow. This method has already been validated against physical models in the laboratory (Fischer-Antze *et al.* 2001), but has not so far been used at the field scale. The method follows the suggestions of the German Association for Hydraulic Engineering (DVWK 1991) and requires a minimum of calibration, since it relates the vegetation geometric properties, including plant diameter and their spacing, to the drag force. To implement the method, geometric vegetation parameters of an existing established floodplain forest were quantified and used as input to the roughness closure model. This was then validated in two stages. First, computed water levels were compared against measured water levels. Second,

Downloaded from https://iwaponline.com/jh/article-pdf/5/2/99/392567/99.pdf
by guest

measurement of the floodplain flow velocity was conducted by dilution gauging to allow the computed floodplain velocities to be verified. This will enable the ability of the model to accurately describe the hydraulic resistance of a vegetated floodplain and describe the fully 3D velocity distribution characteristic for vegetated floodplain flows to be assessed.

NUMERICAL MODEL DESCRIPTION

Discretisation of governing flow equations

The utilised numerical model has been developed and validated at Bristol University on a variety of flow situations in physical models and is fully described by Stoesser (2002). However, a summary of the salient points is given in the following. The program calculates hydrodynamics for a general 3D geometry, discretised by the finite volume method on curvilinear coordinates. The Reynolds averaged Navier–Stokes equations are solved with the continuity equation, written as

$$\frac{\partial U_i}{\partial t} + \frac{\partial U_i}{\partial x_i} = 0 \tag{1}$$

$$\frac{\partial U_i}{\partial t} + U_j \frac{\partial U_i}{\partial x_i} = \frac{1}{\rho} \frac{\partial}{\partial x_i} \left(-P\delta_{ij} - \rho\overline{u_i u_j}\right) + F_D \tag{2}$$

where U is the velocity averaged over time t, x is the spatial geometrical scale, ρ is the water density, P is the pressure, δ is the Kronecker delta and u is the velocity fluctuation in time during the time step dt, when U is subtracted. The second term on the right side of the equation is the Reynolds stress term, which needs to be solved by a turbulence model. The SIMPLEC methods serve as an approach for pressure–velocity corrections and the water level is computed using an interface tracking method. A two-equation standard $k-\varepsilon$ turbulence model is used for calculating the turbulent Reynolds stress term, which has proved its accuracy and reliability in open-channel flows of complex geometry (e.g. Rodi 1980) and for flows through vegetation (e.g. Lopez & Garcia 1997).

Implementation of boundary conditions

To perform a flow simulation, four boundaries need treatment. The inflow boundary is set as a Dirichlet boundary condition: since only the upstream discharge is known it is prescribed at the inlet. At the outflow boundary, neither the value of the flow variable nor the flux is known. Therefore, the water level is kept constant and a zero variable gradient condition (Neumann boundary condition) is used. The water surface is treated as a free surface boundary condition and is modelled with an interface tracking method as described in Stoesser (2002). The impermeable walls in an open-channel flow, i.e. river bed and banks, are described by means of the no-slip condition. However, since the occurrence of steep gradients at this boundary would require a very high grid resolution near the wall, a log-law approach is employed in order to connect the wall shear stresses to the dependent variables. This in turn relies on bed roughness expressed through the equivalent grain roughness k_s (Stoesser 2002). To model the additional flow resistance of submerged or emergent vegetation the drag force on a rigid obstacle has been introduced as a sink term into the Navier–Stokes equations. This term is additional to the bed roughness term. The drag force per fluid mass unit on a vegetative element can thus be calculated as (e.g. Lopez & Garcia, 1997)

$$F_D = \rho \frac{u^2}{2} C_D \lambda \tag{3}$$

where C_D = drag coefficient, set to unity for solid objects of round base shape at high Reynolds numbers and the vegetative coefficient λ is defined as

$$\lambda = \frac{\text{projected area of plant}}{\text{total volume}} = \frac{D}{a_x a_y} \tag{4}$$

where D is the diameter of a plant and a_x and a_y are the lengths of the control volume (see Figure 2). The drag force flow resistance can be discretised in two different manners as illustrated in Figure 3. First, the grid can be constructed around the vegetation elements, such that D, a_x and a_y are directly related to the physical prototype and represent the grid spacing as well as the drag force

Downloaded from https://iwaponline.com/jh/article-pdf/5/2/99/392567/99.pdf
by guest

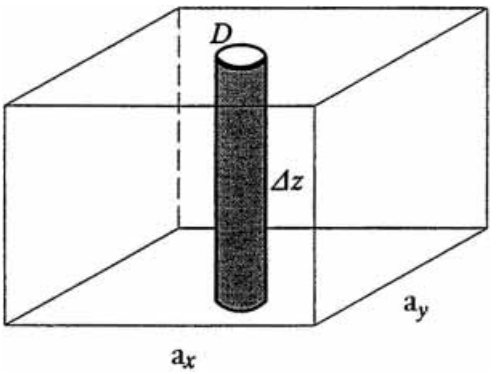

Figure 2 | Notation used in definition of vegetation density λ.

parameters. Second, the grid can be constructed first and the drag force calculated from the parameters D, a_x and a_y as, for example, evaluated in the field. In the second step, as a_x and a_y are already defined through the grid dimensions, the value of vegetation diameter D is varied in order to equal the vegetative coefficient λ from the prototype. This approach was intensively tested by a series of sensitivity tests by Fischer-Antze *et al.* (2001), who showed that the difference between original grid spacing and the application of a variable D is almost negligible (see Figure 3(c)).

To avoid any calibration of simulations for different flow situations, the $k-\varepsilon$ model was not modified and only the Navier–Stokes equations were supplied with a sink term. It was shown in a series of validation test cases with submerged and emergent vegetation (Fischer-Antze *et al.* 2001; Stoesser 2002) that the sink terms are so dominant over the turbulent diffusive terms for natural channel flows that values of k and ε within the vegetation layers did not affect the velocity distribution.

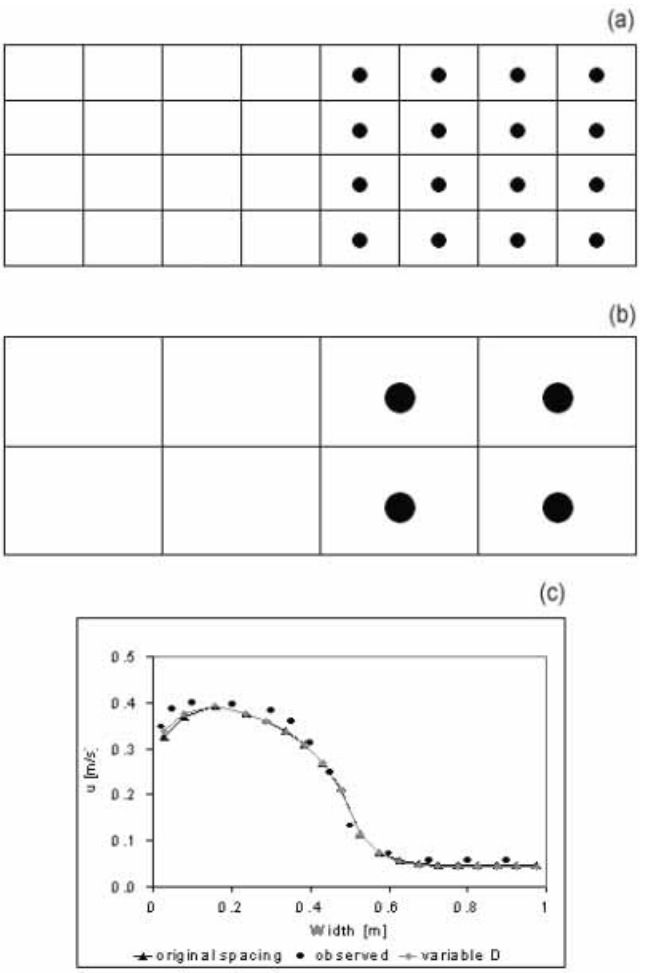

Figure 3 | Drag force discretisation methods. (a) Discretization of grid according to actual vegetation geometry defined by D, a_x and a_y. (b) Parameterization of equivalent vegetation geometry (by setting D to equal the vegetative coefficient λ) following *a priori* discretization of grid grid size defined first. (c) Sensitivity tests performed by Fischer-Antze et al. (2001) in order to test the grid independence of the drag force approach.

DETERMINATION AND CLASSIFICATION OF FLOW RESISTANCE PARAMETERS

The German Association for Hydraulic Engineering (DVWK 1991) recommends a hydraulic resistance method directly based on the drag force approach. It uses the vegetation parameters a_x, a_y and D as defined in Figure 4. An established groin field was used as a reference site in order to quantify the vegetation parameters of the existing plant communities (Dittrich & Hartmann 1998). It is composed of a well-developed riparian forest with a rich mixture of rigid trees and flexible bushes. The vegetation is arranged in strips of different thickness, interspersed with open areas of grass, reeds and nettles. The vegetated strip adjacent to the main channel consists of a dense group of willows. Other species found are cottonwood trees, elm trees, ash trees, privet, elder and blackberry bushes. An area of 77 m × 45 m was surveyed in terms of vegetation

Downloaded from https://iwaponline.com/jh/article-pdf/5/2/99/392567/99.pdf
by guest

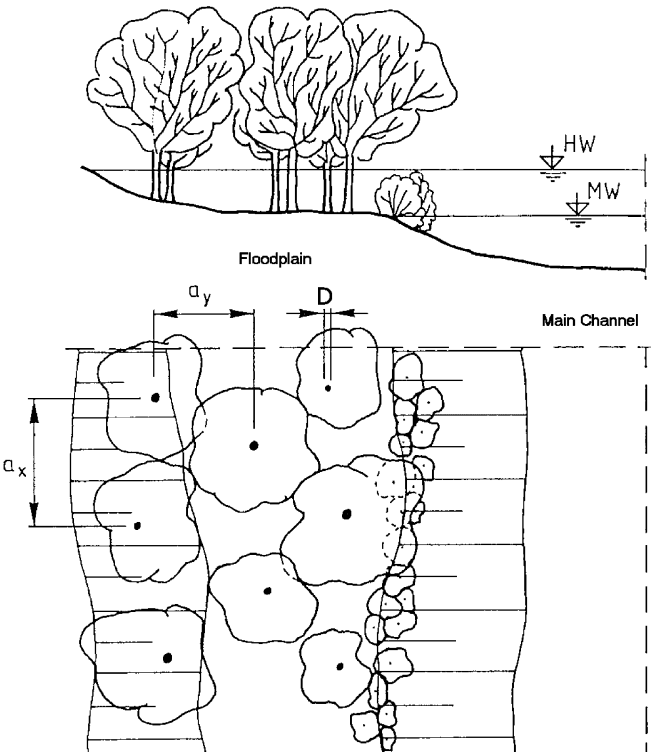

Figure 4 | Characterisation of vegetation parameters a_x, a_y and D (from DVWK 1991).

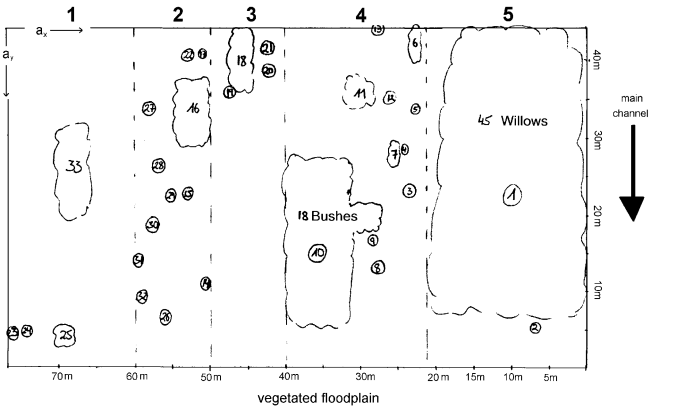

Figure 5 | Quantification of riparian forest vegetation at the test site (Dittrich *et al.* 2000) (strip numbering is given along the top of the diagram).

Table 1 | Summary of vegetation parameters for each monitored strip (see Figure 6 for strip numbering).

Strip no.	1	2	3	4	5	Average
a_x (m)	18.0	4.5	1.1	5.0	20.0	9.7
a_y (m)	3.5	2.0	1.0	3.5	10.0	4.0
D (m)	1.9	1.4	1.5	3.7	13.0	4.3

type and its relative location (see Figure 5). The vegetation varies over the entire monitoring patch and has been classified into five different strips, for which average values of vegetation parameters have been determined (see Figure 5). The patch surveyed is composed of 33 plants and the average vegetative flow resistance parameters per strip that are needed in order to calculate the flow resistance are given in Table 1.

FLOODPLAIN VELOCITY MEASUREMENTS

Velocity measurements are complicated in the case of vegetated floodplains as the plants act as vertical obstructions to the flow. This results in the production of vortices immediately downstream of the vegetational elements and generates a strongly heterogeneous flow field. Hence, dilution gauging methods to determine the mean velocity u_m as a bulk parameter in submerged or emergent vegetation appear to be a good alternative to conventional point velocity measurement methods (e.g. Nepf 1997). However, the presence of recirculation zones behind vegetative elements, that may accumulate the tracer and hence falsify the velocity determination, can be a problem. Therefore the velocity measurements were repeated four times at two different sampling stations (i.e. eight independent measurements), such that a reliable bulk velocity value could be determined.

Floods with a peak discharge of 3600 $m^3 s^{-1}$ occurred on the River Rhine over a period of several months between February and May 1999 as a result of heavy rainfalls and snow melt in the Alps. This corresponds to a flood event of a 100 year return period. For the dilution gauging the tracer used was Uranine, which is green–yellow in appearance. The gulp injection or integration method was employed and the tracer was released from a boat. Three locations in the groin field were selected for the release station, and sampling stations 1 and 2

Downloaded from https://iwaponline.com/jh/article-pdf/5/2/99/392567/99.pdf
by guest

Figure 6 | Field site with sampling stations (SaSt1, SaSt2), release station and surveyed cross sections 191.06 km and 191.29 km marked.

(Figure 6). The injection station and the sampling station 1 (SaSt1) were a distance 54 m apart, whilst the injection station and the sampling station 2 (SaSt1) were a distance 99.5 m apart. Pumps were attached to a rope allowing the water samples to be conveyed through a tube to the floodplain bank. The concentration was sampled at intervals of 10 s for a 10 min period. In order to acquire an accurate measurement of the mean flow velocities, the tracer injection and concentration measurement was repeated four times. The concentration of the tracer samples was measured with a fluorometer and the resulting time series of tracer concentrations for each measurement at the two sampling stations are given in Figures 7(a–d).

The transport of the tracer cloud at each sampling point is clearly visible by the sharp increase and decrease of concentration (see Figures 7(a–d)). The centroid of the time–concentration curve was evaluated in order to estimate the travel times from the injection point to the sampling stations (Table 2). The measurement procedure and the apparatus employed may appear to be

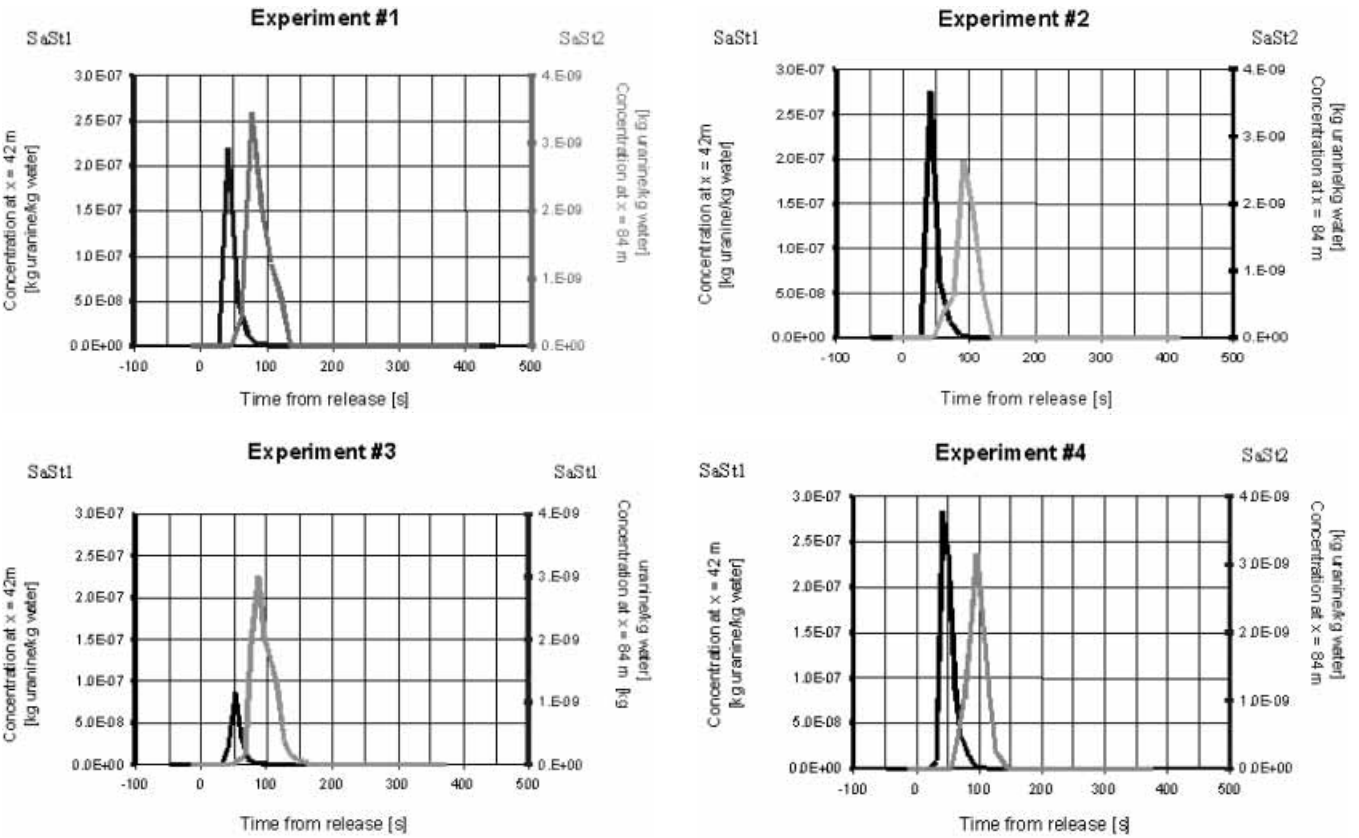

Figure 7 | Temporal tracer concentration at sampling station 1 (black) and sampling station 2 (grey) for the four repeated experiments.

Downloaded from https://iwaponline.com/jh/article-pdf/5/2/99/392567/99.pdf
by guest

Table 2 | Travel times and distances between injection and sampling stations.

Experiment no.	Δt_1 (s)	Δt_2 (s)	Δx_1 (m)	Δx_2 (m)	$\Delta t_2 - \Delta t_1$ (s)	$\Delta x_2 - \Delta x_1$ (m)
1	45.2	88.2	54.0	99.5	42.9	45.5
2	46.0	95.7	54.0	99.5	49.7	45.5
3	45.0	No values	54.0	99.5	—	45.5
4	54.3	95.3	54.0	99.5	41.0	45.5

rudimentary; however, given the difficult working conditions a good estimate of floodplain flow velocities was achieved. The average value of the mean floodplain flow velocity calculated as

$$u_m = \frac{1}{n} \sum_{i=1,n} \frac{\Delta x_i}{\Delta t_i} \tag{5}$$

was evaluated as $u_m \approx 1.1$ m s^{-1} with a standard deviation of 0.07 m s^{-1}.

SIMULATION OF THE 1999 FLOOD

Boundary conditions and set-up

The test reach of the Rhine between km 190.0 and km 193.46 was discretised according to 26 cross sections, which were surveyed in 1986. A relatively high-resolution mesh of 198,144 cells was constructed comprising $258 \times 64 \times 12$ cells in the streamwise, cross-streamwise and vertical directions, respectively (Figure 8). This gives an approximate cell size of 13 m × 3 m × 0.5 m. A summary of the modelled reach details and the numerical set-up are given in Table 3. The grain roughness k_s was calculated from the average gradation curve of the bed material determined through particle sieve analysis (see Figure 9). The equivalent grain roughness height k_s varied in the range 0.31–0.67 m, depending on the formula employed (Table 4). The bed boundary roughness of the river channel was initially set to a roughness height $k_s = 0.45$ m evaluated from $d_m = 0.129$ m following a formula suggested by Dittrich (1998) for a gravel bed river. The floodplain Reynolds number based on the average water depth on the floodplains and the mean floodplain velocity is approximately 3,000,000. The calculations started from a set downstream water level with the given discharge prescribed at the inlet.

RESULTS AND DISCUSSION

Water surface profile

Whilst the aim of the model based here has been to utilise a physically based approach, the parametrisation of grain roughness and vegetation geometry from fieldwork will undoubtedly contain some error. For example, Table 3 demonstrates that, even in this well-defined case where particle sieve analysis has been conducted, the choice of bed roughness value is dependent on the choice of formulae. Hence, to provide increased confidence in the hydraulic resistance values, the bed roughness of the main channel and the form roughness of the vegetated floodplains were independently verified using two different flow conditions. These correspond to flow situations where both the water level observations and discharge measurements were available:

- High flow event on 2 November 1998 where $Q = 700$ m^3 s^{-1}
- Flood event on 29 May 1994 where $Q = 3040$ m^3 s^{-1}

During the 1998 event most of the vegetated floodplains were not inundated, hence this flow condition was used to verify the value of the main channel bed roughness. For this flow the bed friction parameter was calibrated, and an optimum value of $k_s = 0.35$ m, corresponding to a Mannings n of $n = 0.032$, was found. This is equivalent to the value suggested by the Mertens formulae based on the sieve analysis. The difference between calibrated ($n = 0.032$) and uncalibrated ($n = 0.033$) values was thus negligible and good correspondence could be obtained

Downloaded from https://iwaponline.com/jh/article-pdf/5/2/99/392567/99.pdf
by guest

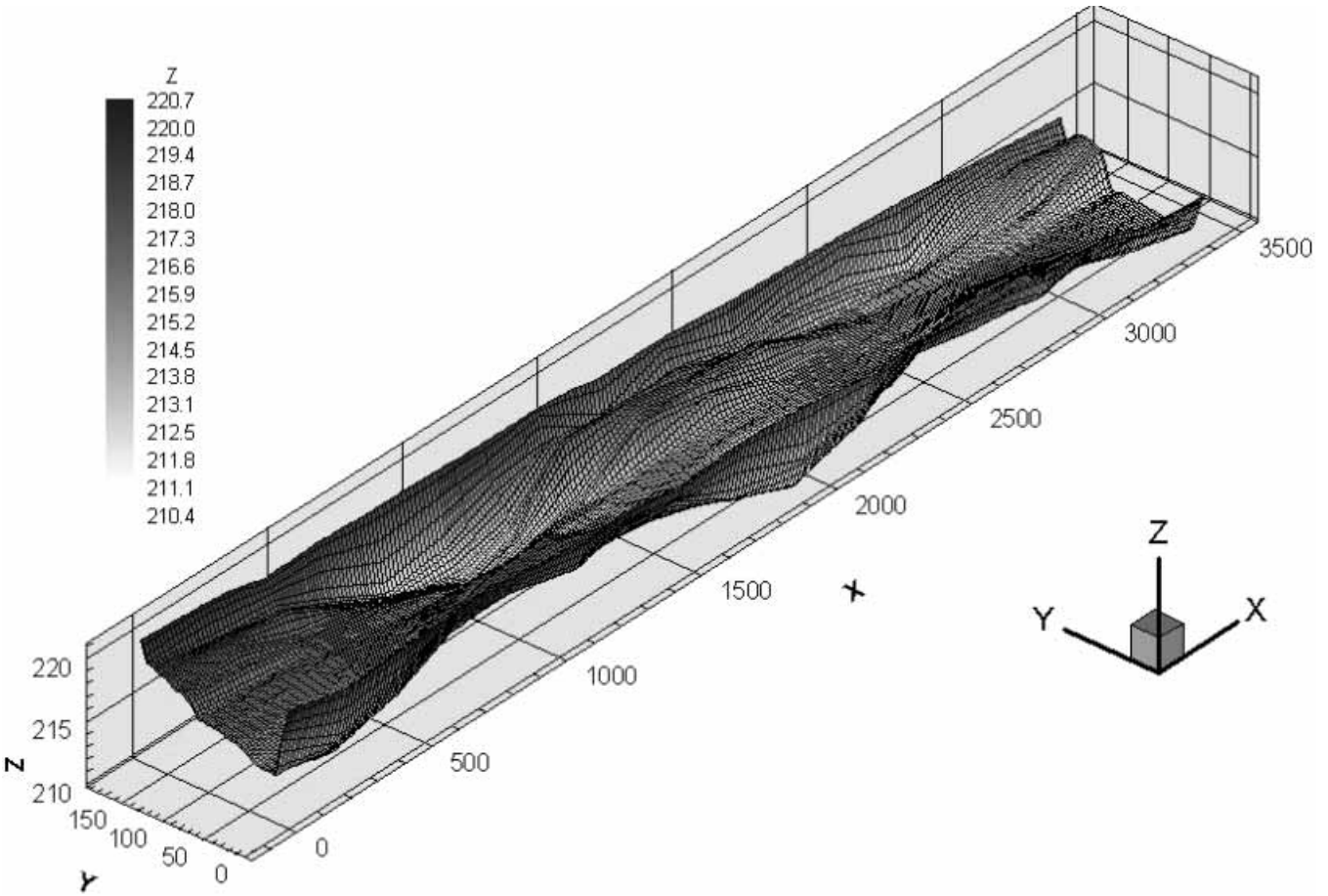

Figure 8 | Computational grid used for the simulations, where *z* is the bed elevation (all dimensions given in metres).

between the measured and computed water surface profiles for this event for both parametrisations (see Figure 10). The vegetative roughness coefficient λ_p was verified using the larger flow event (3040 $m^3 s^{-1}$) where all floodplains were inundated. The parameter λ_p was adjusted from 0.11 l m^{-1} to 0.082 l m^{-1} by the variation of plant diameter D in order to achieve a good match between the observed and computed water levels (see Figure 11). If we assume that the distribution of vegetation is the same as in the reference site (i.e. that a_x and a_y are held constant), this value corresponds to a further reduction in average plant diameter of 4.3 m to 3.2 m. We assume that this need for recalibration is predominately due to errors in determining vegetation geometric and biomechanic properties and indicates the level of precision necessary to achieve these measurements. For the 1994 event the value for bed roughness was parametrised as the calibrated value for the 1999 flood. As Figure 12 shows, the agreement between observed and calculated waterlevels is likewise satisfying. This illustrates that this method requires a minimised calibration effort, since the determination of roughness parameters is based on the physics of the flow resistance.

Flow field

The presence of the vegetated groin fields on alternating sides along the reach causes a reduction in velocity within the floodplain relative to the main channel (see Figures 13 and 14). The computed near-surface velocities are up to

Downloaded from https://iwaponline.com/jh/article-pdf/5/2/99/392567/99.pdf
by guest

Table 3 | Summary of both geometric and flow condition parameters, and simulation details.

Parameter/numerical detail	Units	Value
Length of river reach (m)	(m)	≈3500
Average river width (m)	(m)	≈180
Average channel depth (m)	(m)	≈5.0
Discharge	($m^3\ s^{-1}$)	≈2450, i.e. nearly bankful state
Dynamic viscosity	($kg\ m^{-1}\ s^{-1}$)	1.0×10^{-3}
Floodplain Reynolds number		≈3,000,000
Time step		Steady state
Turbulence closure		$k-\varepsilon$
Roughness closure		Two-layer non-slip + drag force

3.8 m s^{-1} (see Figures 14 and 15). The resultant velocity distributions at selected cross sections in Figure 14 are drawn looking in the upstream direction and are exaggerated in the vertical by a factor of 3. There is a marked reduction in velocity at the main channel/riparian floodplain interface, where floodplain flow velocities are approximately between 1.0–1.5 m s^{-1}. It can be seen that on the floodplain the near-surface velocity distribution is fairly uniform and of the order of 1.0–1.2 m s^{-1}, corresponding well with the measured value from the dilution gauging experiments.

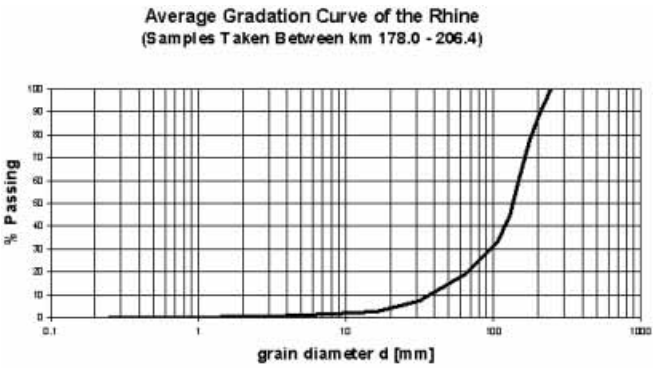

Figure 9 | Average gradation curve of the bed material from the Rhine south of Breisach (km 178–206).

The reduction in velocities due to the vegetated floodplain is further seen in Figure 15. In contrast to the main channel velocity distribution with depth, the floodplain velocity follows a relatively uniform vertical velocity profile. As reported by Raupach & Thom (1981), a vegetation layer can be regarded as analogous to the so-called roughness sublayer, where the velocity distribution is linear. The reason for this is that the flow resistance of emergent vegetation acts over the whole water depth, retarding the flow considerably. This is in agreement with findings from experimental investigations where the velocity profile within both rigid and flexible vegetation layers has been shown to no longer follow the logarithmic law profile (Tsujimoto *et al.* 1992; Nepf & Vivoni 1999).

The cross section at Rhine km 191.29 (see Figure 14(c)) corresponds to the test site in the groin field near Bad Bellingen. Here, a uniformly distributed velocity (over floodplain width and depth) of approximately 1.0 m s^{-1} was computed, which corresponds well with the observed mean velocity from the tracer field tests. Figures 14(a–d) also show the tendency of the relatively straight river reach to meander due to the alternating location of the floodplains and the vegetation on the river banks. There is a trend for the higher velocities to be predicted mainly in the deeper parts of the main channel.

Downloaded from https://iwaponline.com/jh/article-pdf/5/2/99/392567/99.pdf
by guest

Table 4 | Grain roughness and Strickler value of main channel as suggested by different authors, where n refers to Manning's n value.

	d (mm)	Author	Formula	k_s (m)	n (s m$^{-1/3}$)
d_{65}	155	Engelund & Hansen (1967)	$k_s = 2d_{65}$	0.310	0.031
d_{50}	136	Mertens (1994)	$k_s = 2.5d_{50}$	0.340	0.032
d_m	129	Dittrich (1998)	$k_s = 5.5d_m$	0.451	0.033
d_{84}	192	Hey (1979)	$k_s = 3.5d_{84}$	0.672	0.036

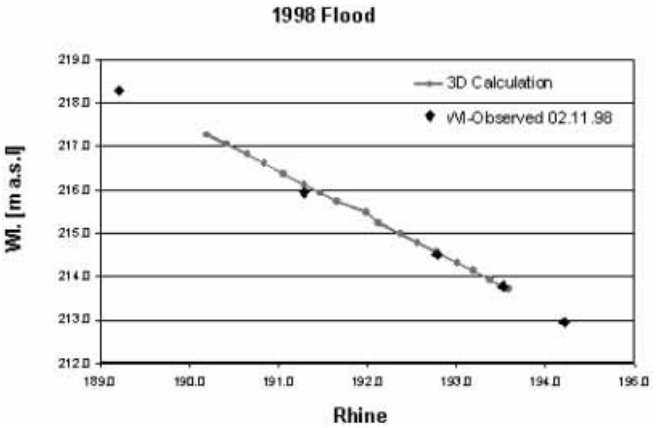

Figure 10 | Comparison of observed and computed water surface elevation after the main channel bed roughness was calibrated for the 700 m^3 s^{-1} flood event in 1998.

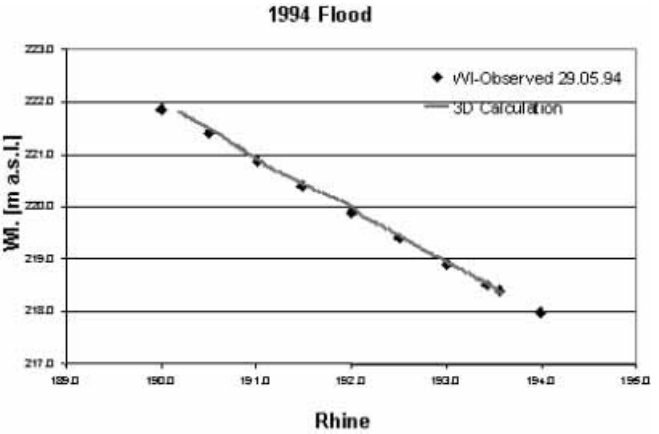

Figure 11 | Comparison of observed and computed water surface elevation after the floodplain vegetative parameters was calibrated for the 3050 m^3 s^{-1} flood event in1994.

Figure 15(a–d) show the distribution of the kinetic energy, defined as $k = \frac{1}{2}\overline{u_i u_i}$ in selected cross sections along the modelled reach. Relatively higher magnitudes of turbulent kinetic energy can be observed in the main channel, while at the main channel/floodplain interface there is a decrease in kinetic energy due to the sudden reduction in velocities induced by the presence of vegetation. The highest turbulent kinetic energy can be seen near the bed in the main channel where the higher velocities are responsible for the bed-load transport processes and formation of an armored layer. Here, the maximum kinetic energy, which corresponds to a maximum shear stress of 57 N m^{-2}, would initiate the motion of sediments up to a size of 70 cm. This is based on the Shields diagram for a non-armored bed with a fairly steep sieve curve (Dittrich 1998). A field visit after the 1999 stormwater event showed that the main channel bed had been in motion and that geomorphological changes in the main channel and along the floodplain interface had indeed taken place (Dittrich *et al.* 2000).

CONCLUSIONS

Whilst the roughness closure approach presented herein does not eliminate entirely the process of calibration, we have presented and applied a method which is based on the physics of flow resistance which significantly reduces

Downloaded from https://iwaponline.com/jh/article-pdf/5/2/99/392567/99.pdf
by guest

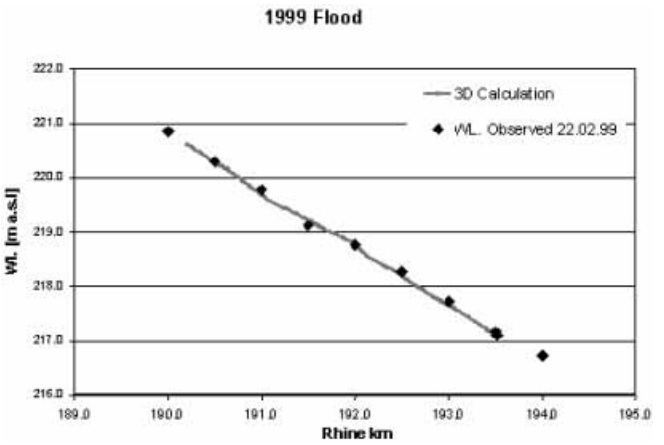

Figure 12 | Independent verification of the computed water surface elevation against the observed water surface elevation for 2400 $m^3 s^{-1}$ flood event in 1999 using the calibrated parameters obtained for the 1994 and 1998 events.

the modelling uncertainties associated with traditional methods of calibration. Previously this method has been tested within the laboratory context and has rarely been used within the complexities of the field environment. A 100 year flood event on a considerable reach length was simulated. Mean floodplain velocities were measured using dilution gauging techniques and good agreement was found between the measured and computed floodplain velocities. Given information such as vegetation distribution/density and planview geometric properties of the vegetation, the proposed eco-hydraulics tool can predict floodplain velocities, water elevation and hydrodynamic features indicative of vegetated two-stage channel flow.

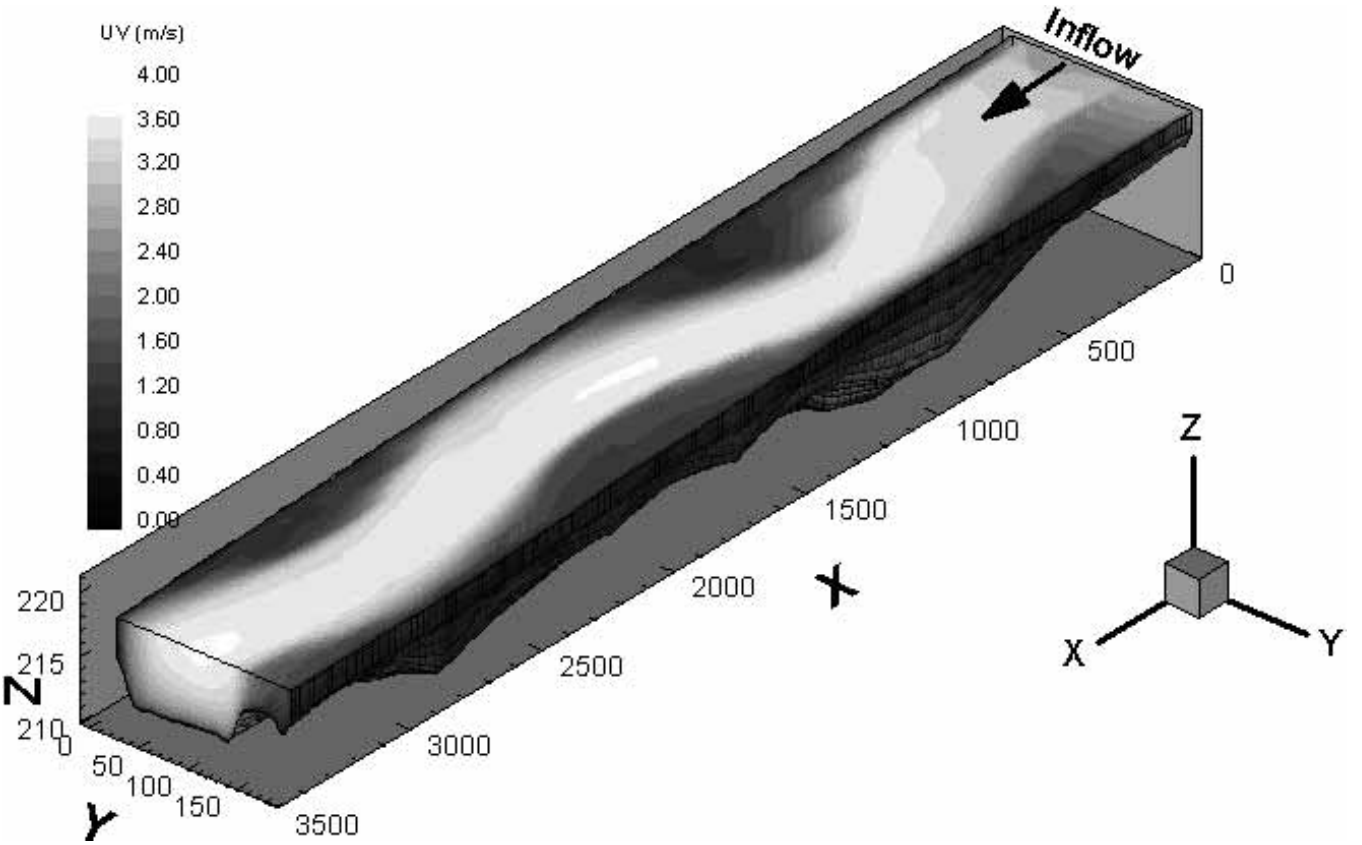

Figure 13 | Flow velocities of the River Rhine Reach (length scales given in metres).

Downloaded from https://iwaponline.com/jh/article-pdf/5/2/99/392567/99.pdf
by guest

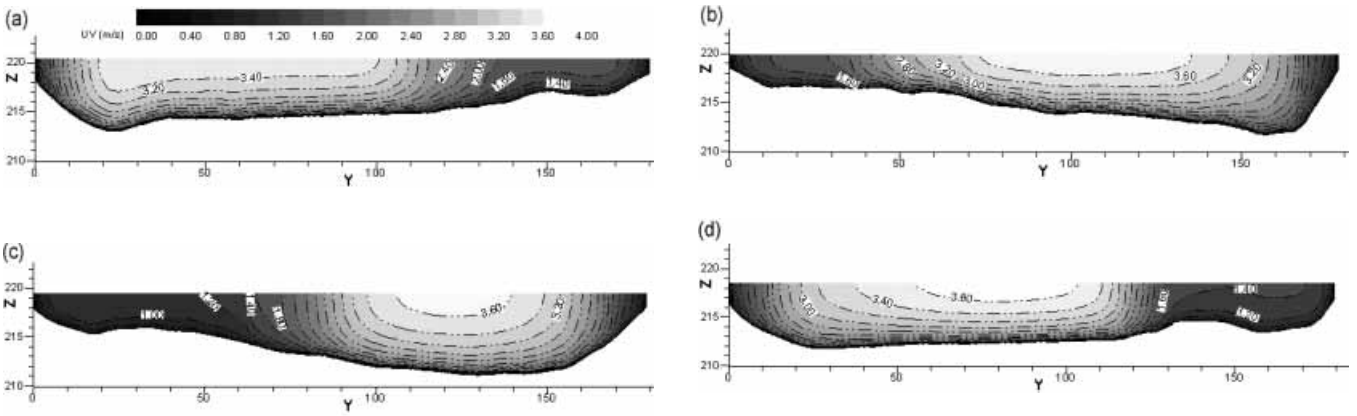

Figure 14 | Cross-sectional distribution of resultant velocity in cross sections: (a) Rhine km 190.42, (b) Rhine km 190.84, (c) Rhine km 191.29, (d) Rhine km 191.94 (all length scales in metres).

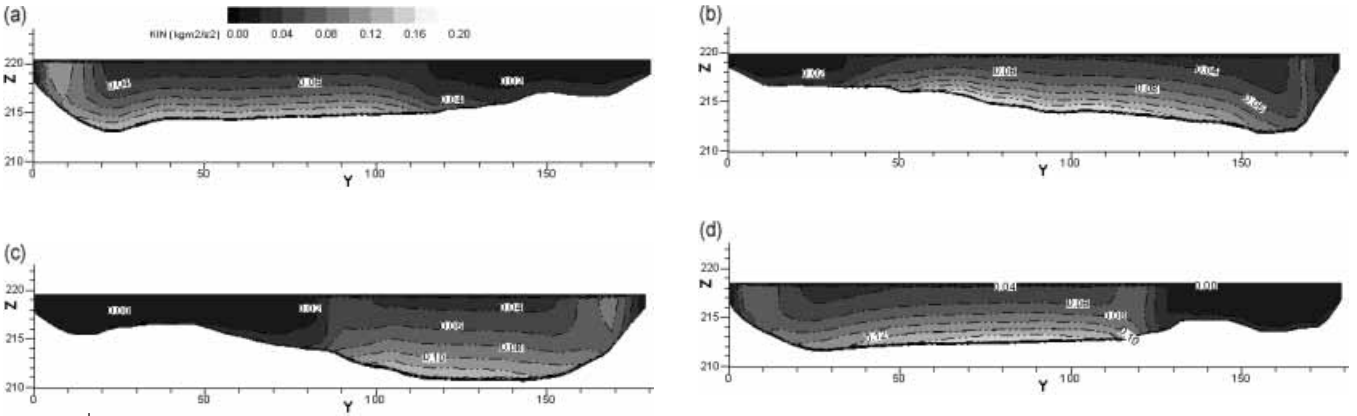

Figure 15 | Cross-sectional distribution of kinetic energy in cross sections: (a) Rhine km 190.42, (b) Rhine km 190.84, (c) Rhine km 191.29, (d) Rhine km 191.94 (all length scales in metres).

NOTATION

C_D	drag coefficient
D	diameter of a plant
a_x	charactristic distance between plants in streamwise direction
a_y	charactristic distance between plants in cross-streamwise direction
δ	Kronecker delta
k	turbulent kinetic energy
P	pressure
t	time
U	average velocity in time
u	velocity fluctuation
x	spatial geometrical scale
ε	turbulent diffusion
λ	vegetative coefficient
ρ	water density

REFERENCES

Choi, S.-U. & Kang, H. 2001 Reynolds stress modeling of vegetated open channel flows. *29th IAHR Congress Conference Proceedings. Beijing, China*. Tsing Hua University Press, China, 264–269.

Chow, V. T. 1959 *Open Channel Hydraulics*. McGraw-Hill, New York.

Cowan, W. L. 1956 Estimating hydraulic roughness coefficients. *Agric. Engng.* **37**(7), 473–475.

Downloaded from https://iwaponline.com/jh/article-pdf/5/2/99/392567/99.pdf
by guest

Dittrich, A. 1998 *Wechselwirkung Morphologie/Strömung naturnaher Fliessgewässer. Habilitationsschrift*. Mitteilungen des Institutes fuer Wasserwirtschaft und Kulturtechnik. No. 198. Universität Karlsruhe.

Dittrich, A. & Hartmann, G. 1998 *Untersuchungen zum Vorlandabtrag zwischen Maerkt und Karpfenhod.* Schlussbericht. Institut für Wasserwirtschaft und Kulturtechnik. Universität Karlsruhe.

Dittrich, A., Hartmann, G. & Träbing, K. 2000 *Rückhalteraum Weil-Breisach Bewertung der morphologischen und hydraulischen Auswirkungen der Hochwasserereignisse 1999 im Rhein zwischen Maerkt und Breisach. Teil B. Analyse und Dokumentation der morphologischen Veraenderungen infolge des Hochwassers Mai 1999.* Schlussbericht. Institut für Wasserwirtschaft und Kulturtechnik. Universität Karlsruhe.

DVWK 1991 *Hydraulische Berechnung von Flie gewaessern.* Merkblaetter. 220/1991. Verlag Paul Parey, Hamburg.

Ervine, D. A. & Ellis, J. 1987 Experimental and computational aspects of overbank floodplain flow. *Trans. R. Soc. Edin. Earth Sci.* **78**, 315–325.

Fischer-Antze, T., Stoesser, T., Bates, P. B. & Olsen, N. R. 2001 3D numerical modelling of open-channel flow with submerged vegetation. *J. Hydraul. Res.* **39**(3), 303–310.

Greenhill R. K. & Sellin R. H. J. 1993 Development of a simple method to predict discharges in compound meandering channels. *Proc. Inst. Civil Engrs. Wat. Maritime Energy* **101**, 37–44.

Hey, R. D. 1979 Flow resistance in gravel bed rivers. *Proc. ASCE J. Hydraul. Div.* **105**(4), 365–379.

Lopez, F. & Garcia, M. 1997 *Open Channel Flow Through Simulated Vegetation: Turbulence Modelling and Sediment Transport.* Hydrosystems Laboratory, Department of Civil Engineering, University of Illinois.

Masterman, R. & Thorne, C. R. 1992 Predicting influence of bank vegetation on channel capacity. *J. Hydraul. Eng.-ASCE* **118**(7), 1052–1058.

Mertens, W. 1994 Zum Strömungswiderstand naturnaher Flie *gewässer. Wasserwirtschaft* **84**(3), 138–141.

Nepf, H. & Vivoni, E. R. 1999 Turbulence structure in depth-limited vegetated flow: transition between emergent and submerged regimes. In *28th IAHR Congress Conference Proc., Graz, Austria*. On CD-ROM.

Nepf, H. M. 1997 Drag, turbulence, and diffusion in flow through emergent vegetation. *Wat. Res. Res.* **35**, 479–489.

Petryk, S. & Bosmajian, G. 1975 Analysis of flow through vegetation. *J. Hydraul. Engng.* **101**(7), 871–884.

Raupach, M. R. & Thom, A.S. 1981 Turbulence in and above plant canopies. *Annu. Rev. Fluid Mech.* **13**, 97.

Rodi, W. 1980 *Turbulence models and their application in hydraulics. A state of the art review.* IAHR, Delft, The Netherlands.

Shimizu, Y. & Tsujimoto, T. 1994 Numerical analysis of turbulent open channel flow over a vegetation layer using a k–ϵ turbulence model. *J. Hydrosci. Hydraul. Engng.* **11**(2), 57–67.

Stoesser, T. 2002 Development and validation of a CFD code for open-channel flows. *PhD Thesis*. Department of Civil Engineering, University of Bristol.

Tsujimoto T., Shimizu Y., Kitamura T. & Okada T. 1992 Turbulent open-channel flow over bed covered by rigid vegetation. *J. Hydrosci. Hydraul. Engng.* **10**(2), 13–25.

Tsujimoto, T., Shimizu, T. & Okada, T. 1991 Turbulent structure of flow over rigid vegetation-covered bed in open channels. *KHL Progressive Report 1*. Hydraulic Laboratory, Kanazawa University, Japan.

Wilson, N. R. & Shaw, R. H. 1977 A higher order closure model for canopy flow. *J. Appl. Meteorol.* **16**, 1198ff.

Wormleaton, P. R., Allen, J. & Hajipanos, P. 1982 Discharge assessment in compound channel flow. *ASCE J. Hydraul. Div.* **108**, 975–994.

Downloaded from https://iwaponline.com/jh/article-pdf/5/2/99/392567/99.pdf
by guest